pansions and intrafacial tension gradients. In one analytical study of the effect of volume expansions on heat transfer in an ideal gas under zero-gravity conditions Larkin concluded that the heat transfer was greatly increased over what would be predicted if such thermally induced motion were neglected (*7*). The term "intrafacial tension" is used to describe a developed tension arising in heated portions of a gas or liquid. Possibly the differences in physical properties between the hot and colder portions of a fluid can be large enough to result in an intrafacial tension. Evidence for this kind of tension has been discussed (*8*).

The demonstration of convection driven by surface tension in low-gravity environments suggests that in feasibility studies for a number of proposed space manufacturing processes in which sizable free liquid surfaces are in direct contact with a gas or vapor phase this sort of convection should be taken into account. The evidence obtained in the radial heating and zone heating experiments for still another form of low-gravity convection requires confirmation.

Further details of these experiments and the data analyses are given elsewhere (*9*).

PHILOMENA G. GRODZKA
Lockheed Missiles & Space Company, Inc., Huntsville, Alabama 35807
TOMMY C. BANNISTER
National Aeronautics and Space Administration, Marshall Space Flight Center, Alabama 35812

References and Notes

1. H. Bénard, *Ann. Chim. Phys.* **23**, 62 (1901).
2. Lord Rayleigh, *Phil. Mag.* **32** (Ser. 6), 529 (1916).
3. M. J. Block, *Nature* **178**, 650 (1956).
4. J. R. A. Pearson, *J. Fluid Mech.* **4**, 489 (1958).
5. E. L. Koschmieder, *ibid.* **30**, 9 (1967); D. A. Nield, *ibid.* **19**, 341 (1964); L. E. Scriven and C. V. Sternling, *ibid.*, p. 321; K. A. Smith, *ibid.* **24**, 401 (1966).
6. S. Ostrach, *Trans. Amer. Soc. Mech. Eng.* **79**, 302 (1957).
7. B. K. Larkin, *Progr. Astronaut. Aeronaut.* **20**, 819 (1967).
8. J. H. Kimzey, *Nat. Aeronaut. Space Admin. Rep. TM-X-53993* (1971), p. 329.
9. T. C. Bannister, "Heat Flow and Convection Demonstration (Apollo 14)," summary report, parts I and II (NASA Marshall Space Flight Center, Alabama, 1971); P. G. Grodzka, C. Fan, R. O. Hedden, *Lockheed Missiles Space Co. Rep. LMSC-HREC D225333* (1971).
10. We are grateful to the many people who were involved in the fabrication, design, and data analysis of these experiments, especially Col. S. A. Roosa for his competent performance of experiments under space conditions. We also thank Dr. J. Bredt for suggesting the use of liquid crystals to track convection isotherms and Dr. E. L. Koschmieder for his many helpful suggestions on the writing of this report. Supported by NASA contract NAS8-25577.

1 October 1971; revised 1 March 1972

Pollution Monitor for Nitric Oxide: A Laser Device Based on the Zeeman Modulation of Absorption

Abstract. *The concentration of nitric oxide can be monitored by a new device in which the Zeeman effect is used to shift an absorption line of nitric oxide into coincidence with a laser line of carbon monoxide. The absorption is modulated by a small, oscillating magnetic field. This device is specific for nitric oxide and is not subject to interference from other gases.*

A new device, using the Zeeman effect, has been devised for the measurement of NO (and possibly NO_2) concentrations in gaseous samples. This device employs a CO laser source at a fixed infrared frequency and employs the Zeeman effect both to tune and to modulate the absorption. It is specific for a strongly paramagnetic substance such as NO and is not subject to interference from other contaminants in the sample, since other contaminants either have magnetic moments too small to modulate significantly (for example SO_2 and H_2O) or do not absorb infrared radiation (O_2). Because of the wide separation of the NO and NO_2 absorption bands, an excess of NO_2 does not interfere with the measurement of NO concentrations.

Kreuzer and Patel (*1*) have explained the need for an improved NO detector and have also outlined the problems involved in using infrared absorption to measure the concentrations of pollutants. They have shown how a tunable spin-flip Raman laser can be coupled with an optoacoustic detector to measure low concentrations of NO in the presence of other contaminants. Such continuously tunable laser devices are expensive and require skilled operators. Consequently, it is desirable to explore the possibility of developing simpler and cheaper measurement devices. Past attempts to utilize fixed-frequency lasers have not been notably successful because pressure broadening is usually required to achieve sufficient overlap of the absorption line of the pollutant and the laser line. This has two consequences: (i) measurements with a single laser line are no longer adequate to identify the pollutant, and (ii) moderate concentrations or long path lengths are required to obtain sufficient absorption. For NO we have overcome these difficulties by using the Zeeman effect to shift the absorption into near coincidence with a CO laser line and to modulate the molecular absorption line rather than the incident laser light.

Our device consisted of a continuous-wave CO laser oscillating only on the 1884.37-cm^{-1} line, an absorption cell placed between the pole pieces of an electromagnet, and an infrared detector to monitor the intensity of the laser radiation after it passed through the absorption cell. A d-c magnetic field was used to shift the Zeeman components of the NO absorption line into near coincidence with the CO laser line. The modulated magnetic field which was used to modulate the Zeeman components of the molecular absorption line in and out of resonance with the CO laser line was generated by using an audio amplifier to drive a set of small coils attached to the pole pieces of the electromagnet. The resulting modulated signal from the infrared detector was measured with a lock-in amplifier. In our experiments the field was modulated with the frequency 1 khz, and the amplitude of modulation was varied from 10 to 100 gauss. Measurements were made in the pressure range 1 to 30 torr. In the configuration described above the absorption cell is outside the laser cavity. With an intracavity configuration the device would be more sensitive to the presence of NO at very low concentrations but would probably be less able to quantitatively measure NO over a range of concentrations.

We now examine briefly conditions governing optimum values for the static and alternating magnetic fields. Qualitatively, one expects the intensity of the first-derivative spectrum to be greatest if (i) the sharp laser line lies on the steepest part of the much broader absorption line, and (ii) the modulating magnetic field shifts the line by half the line width in each direction. Quantitatively, the intensity of the first-derivative spectrum for low absorption (no saturation) and low pressure (Doppler line shape) is proportional to the Fourier coefficient of the $\cos\omega t$ term in the expression

$$\sigma^{-1} \exp\left[-1/2\left(\frac{d}{\sigma} + \frac{a}{\sigma}\cos\omega t\right)^2\right] \qquad (1)$$

where σ is the full width of the absorption line at half intensity in wave numbers (cm^{-1}) divided by the factor

$(8 \ln 2)^{1/2} \cong 2.35$, ω is the frequency of the oscillating magnetic field, and t is time. The parameter d is the separation in wave numbers of the laser line from the line center of the Zeeman component and for optimum signal is expected to have the value σ. The parameter a is the modulation amplitude of the absorption line in wave numbers. It can be seen, by expanding the expression above as a power series in the parameter a/σ, that the Fourier coefficient governing the intensity of the first-derivative spectrum is given by

$$\sigma^{-1} \exp[- 1/2(d/\sigma)^2]\{-(d/\sigma)(a/\sigma) + 1/8[3(d/\sigma) - (d/\sigma)^3](a/\sigma)^3 + 0(a/\sigma)^5\} \tag{2}$$

From this expression we see that for small a/σ (that is, for easily obtainable modulating magnetic fields) the intensity of the derivative spectrum is proportional to the modulation amplitude a and reaches a maximum value for $d \cong \sigma$. Numerical calculations based on Eq. 1 show that the maximum intensity of the first-derivative spectrum is achieved for a/σ near 1.9. In our experiments we have varied a/σ from 0.1 to 1.5 and have observed the expected improvement in sensitivity.

In order to optimize the sensitivity of this device for a small fixed amplitude of modulation, we chose to examine the NO transition having the largest product of intensity (I) times the Zeeman shift coefficient ($\Delta\nu/H$). Only the low J transitions of the $^2\Pi_{3/2}$ state of NO show large Zeeman shifts. Of these only the $J = 5/2 \leftarrow 3/2$, $\nu = 1 \leftarrow 0$ transition at about 1884.32 cm^{-1} (*2*) lies close to a CO laser line, that is, the ($\nu = 9 \rightarrow 8$) $P(13)$ line at 1884.37 cm^{-1} (*3*). (Our measurements show that the actual separation of these lines is about 0.028 cm^{-1}.) In a magnetic field the $J = 5/2 \leftarrow 3/2$ transition splits into 12 electric-dipole allowed transitions symmetrically displaced (to first order) from the zero-field transition. Four of these are $\Delta M = 0$ transitions in which light polarized parallel to the magnetic field is absorbed (as in our experimental configuration) while the remaining eight are $\Delta M = \pm 1$ transitions in which perpendicularly polarized light is absorbed.

The calculated relative intensities (I), Zeeman shift coefficients ($\Delta\nu/H$), field required to shift the Zeeman component into coincidence with the laser line (H_c), and modulability [$I \cdot (\Delta\nu/H)$] are given in Table 1 for those transitions which can be shifted into coincidence with the CO laser line. From this table it is obvious that the most sensitive transition to use for small modulating magnetic fields is the $M = +3/2 \leftarrow +3/2$ transition.

Table 1. Relative intensities (I), Zeeman shift coefficients ($\Delta\nu/H$), field (H_c) required for coincidence with the laser line, and relative intensity [$(I) \cdot (\Delta\nu/H)$] of the ($a/\sigma \ll 1$) derivative spectrum for the Zeeman components of the $\nu = 1 \leftarrow 0$, $J = 5/2 \leftarrow 3/2$ transition of the $^2\Pi_{3/2}$ state of NO.

Zeeman component $M' \leftarrow M''$	I	$\Delta\nu/H$ (cm^{-1}/kgauss)	H_c (kgauss)	$I \cdot (\Delta\nu/H)$ (normalized)
$+3/2 \leftarrow +3/2$	16	3.22×10^{-3}	0.90	1.00
$+1/2 \leftarrow +1/2$	24	1.07×10^{-3}	2.70	0.50
$+5/2 \leftarrow +3/2$	20	1.74×10^{-3}	1.66	0.68
$+3/2 \leftarrow +1/2$	12	0.41×10^{-3}	7.14	0.09
$-1/2 \leftarrow +1/2$	6	2.55×10^{-3}	1.14	0.30
$+1/2 \leftarrow +3/2$	2	4.70×10^{-3}	0.62	0.18

In Fig. 1, a and b, we show the derivative spectrum and absorption curve of the $\Delta M = 0$ transitions in NO, obtained with the CO laser, as the magnetic field is swept from 0 to 4000 gauss. In Fig. 1, c and d, we show predicted positions and intensities for the absorption spectrum associated with $\Delta M = 0$ and $\Delta M = \pm 1$ transitions, respectively. Figure 1a verifies the prediction in Table 1 that the maximum intensity of the derivative spectrum for the $M = +3/2 \leftarrow +3/2$ transition is greater than that for the $M = +1/2 \leftarrow +1/2$ transition; in the limit of infinitesimal modulating field the ratio would be 2/1. Since the Zeeman shift coefficient for the $M = 3/2 \leftarrow 3/2$ transition is three times larger than for the $M = 1/2 \leftarrow 1/2$ transition, the ratio of the apparent integrated intensities of the two peaks in Fig. 1b is three times larger than the ratio of the intensities shown in Fig. 1c (and given in Table 1).

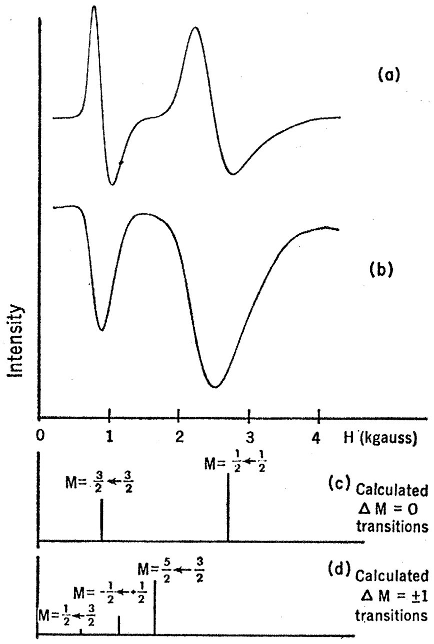

Fig. 1. (a) Observed derivative spectrum of NO at 0.5-torr pressure and 20-cm path length, (b) observed absorption spectrum at 2-torr pressure and 20-cm path length, (c) calculated position and intensity of the absorption spectrum for $\Delta M = 0$, and (d) calculated position and intensity of the absorption spectrum for $\Delta M = \pm 1$.

In order to determine the sensitivity of our device we made measurements on laboratory samples with known concentrations of NO (prepared by successive dilution with nitrogen gas to avoid the reaction with O_2 in air at high NO concentrations). We were able to measure 60 parts per million of NO with a signal-to-noise ratio of 70, and from the results we extrapolated to a sensitivity of 3 ppm. Measurements on automobile exhaust were also performed with a good signal-to-noise ratio.

Since the infrared absorption of H_2O appears to overlap that of NO in low-resolution spectra, we have considered several ways in which H_2O might interfere with the NO measurements, but none of them can significantly reduce the sensitivity of this device until one approaches the range of parts per billion. For example, the attenuation of the laser beam by H_2O is not a problem for the laser transition used here. Modulation of the H_2O absorption by means of the Zeeman effect in H_2O is not large enough to interfere with the measurement of NO since the Zeeman shift coefficient for H_2O transitions is 10^{-4} times as large as that for the NO transition and the nearest H_2O line is 0.20 cm^{-1} (more than ten line widths) from the laser line. Our calculations indicate that H_2O will not cause any trouble at concentrations greater than 1 ppb of NO.

The prototype instrument described in this report can be further refined to improve its sensitivity. The absorption path can be increased by at least an order of magnitude if a multiple-reflection absorption cell is used. With this improvement and improvements in the detector and the laser stability, the device should be able to quantitatively measure NO concentrations to better than 0.1 ppm. With an intracavity configuration the sensitivity of the device can be extended to the range of parts per billion.

ANDREW KALDOR
WM. BRUCE OLSON, ARTHUR G. MAKI
National Bureau of Standards,
Washington, D.C. 20234

References and Notes

1. L. B. Kruezer and C. K. N. Patel, *Science* 173, 45 (1971).
2. T. C. James and R. J. Thibault, *J. Chem. Phys.* 41, 2806 (1964).
3. A. W. Mantz, E. R. Nichols, B. D. Alpert, K. N. Rao, *J. Mol. Spectrosc.* 35, 325 (1970).
4. We thank Dr. Jon Hougen for discussion and helpful advice on the theoretical aspects, and Drs. K. Evenson and B. Woodward for helpful advice on some experimental aspects of this work. Supported in part by the Measures for Air Quality Office of the National Bureau of Standards. A.K. is a National Bureau of Standards–National Research Council postdoctoral research associate.

10 November 1971; revised 1 March 1972 ■

Lead Isotopes in North American Coals

Abstract. *Lead isotopes in North American coals are equally or much more radiogenic than those in the present continental crust (a mean composition for the continental crust is used). It is practicable to distinguish coal and gasoline lead pollutants by examining their isotopic compositions.*

Atmospheric lead pollution is well documented (*1*), and the ambient lead concentrations are far above those naturally occurring (*2*). In 1968 an estimated 184,316 tons of lead aerosols were emitted in the United States. Of this, some 181,000 tons of lead were attributed to the combustion of leaded gasoline, and 920 tons were attributed to coal burning, the second largest emission source. In regions where coal burning prevails, studies have indicated lead concentrations as high as 150 ppm in fly ash and 358 ppm in soot near coal-burning electric power plants (*3*).

Each natural lead deposit has a characteristic isotopic composition, and this unique property has been used to trace lead pollutants in the environment (*4*). The isotopic compositions of coal leads may make it possible to differentiate the sources of emission.

Coal samples were obtained from various North American coal provinces. Coals of the Eastern and the Interior provinces were deposited during the Pennsylvanian age, those of the Rocky Mountain province during the Mesozoic age, and those of the Great Plains and the Pacific Coast provinces during the Tertiary age.

The washed coal samples were pulverized to 100 to 200 mesh size, weighed, and ashed at 400°C to constant weight. The lead was extracted by treating the ash with concentrated nitric and perchloric acids, isolated by standard ion-exchange technique, purified by several dithizone extractions, and then converted to the sulfide form for isotopic analysis. Mass spectrometry was performed with a solid-source instrument (radius 30 cm) with an electron multiplier. Corrections proportional to the square root of the mass ratio are incorporated in the data to compensate for velocity discriminations in the electron multiplier. The following limits (90 percent confidence interval) were assigned to the lead isotope ratios: ± 0.3 percent of the $^{206}Pb/^{204}Pb$ ratio, ± 0.1 percent of the $^{206}Pb/^{207}Pb$ ratio, and ± 0.2 percent of the $^{206}Pb/^{208}Pb$ ratio.

We have determined the lead contents of 143 coal samples, which contain an average of 11 ppm of lead (96 ppm on an ashed basis). The details of the lead concentration data will be discussed elsewhere. Some 21 samples were selected and analyzed for their lead isotopic composition (Table 1). The isotope ratios show that coal leads are equally or much more radiogenic than the average lead in the present continental crust. Lead isotope ratios in the continental crust, based on analysis of marine sediments, are 18.45 for $^{206}Pb/^{204}Pb$ and 1.182 for $^{206}Pb/^{207}Pb$ (*5*). The isotopic composition of the lead in the coal samples showed no correlation with the age of plant accumulation or coalification. However, the radiogeneity of the lead in the coal is inversely proportional to the lead concentration. This is evidenced by coal samples 62, 81, 83 and USBM-1 (Table 1), which contain high lead concentrations (between 33 and 170 ppm) and the least radiogenic lead. This can be explained by the gradual accumulation

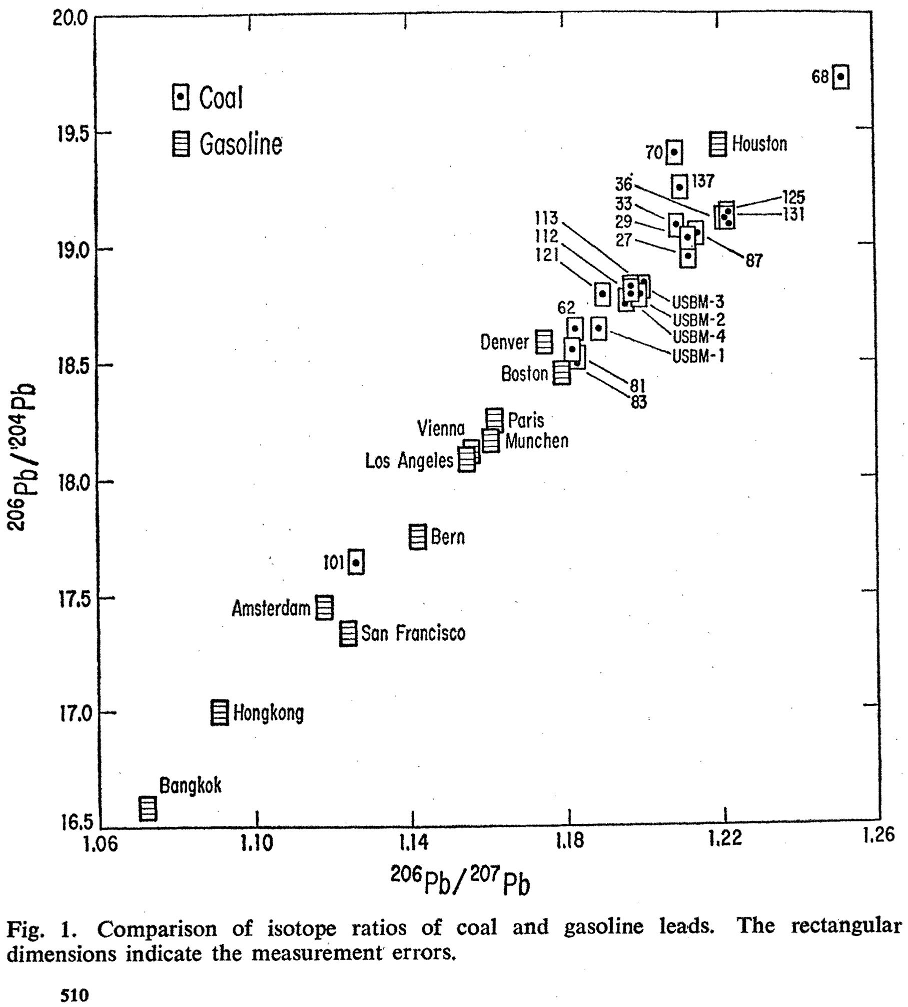

Fig. 1. Comparison of isotope ratios of coal and gasoline leads. The rectangular dimensions indicate the measurement errors.